

SIMULATION OF TRANSVERSE SINGLE BUNCH INSTABILITIES AND EMITTANCE GROWTH CAUSED BY ELECTRON CLOUD IN LHC AND SPS.

E. Benedetto*, D. Schulte, F. Zimmermann, CERN, Geneva, Switzerland
G. Rumolo, GSI, Germany

Abstract

The electron cloud may cause transverse single-bunch instabilities in proton beams such as those in the LHC and the CERN SPS. These instabilities and the consequent emittance growth are simulated by the HEADTAIL code with conducting boundary conditions. The sensitivity of the simulation results to several numerical parameters is studied by varying the number of interaction points of the bunch with the cloud, the phase advance between subsequent interaction points and the number of macroparticles used to represent the protons and the electrons. Simulations for the SPS, including a transverse feedback system and a dipole magnetic field, can be used to benchmark the code with machine observations. The effects of a large chromaticity on the instability evolution are investigated for both SPS and LHC, considering various levels of electron cloud density. An attempt is made to extrapolate to low electron densities. We also compare the initial instability rise times with those obtained for an equivalent broadband resonator.

INTRODUCTION

Instabilities, beam loss and beam size blow up due to electron cloud have been observed in several machines (CERN PS and SPS, KEKB, LER, PEP2) and can be a concern for the future Large Hadron Collider (LHC) at CERN. In this paper we discuss simulations of transverse single-bunch instabilities using the code HEADTAIL [1] which has been developed at CERN.

During the passage of a bunch, the electrons are accumulated around the beam center (pinch effect) and, if the head of the bunch is slightly offset, the rest of the bunch will experience a net "wake" force. The instability is similar to the regular transverse mode coupling instability (TMCI) and induces both a centroid and an head-tail motion, with a substantial emittance growth.

HEADTAIL is a PIC code which models the interaction of a single bunch with an electron cloud on successive turns, with the simplification that the cloud is localized at a finite number of positions along the circumference, instead of being continuously spread over the entire ring. Recently, electric conducting boundary conditions (b.c.) have been implemented into the code [2]. They replaced the previous open space boundaries. A description of these will be given in the next section. The sensitivity of the code to

numerical parameters, in particular to the number and location of the Interaction Points (IPs) between the cloud and the bunch will be discussed in the following section. Then simulations results for LHC and SPS will be shown. We here investigate the instability threshold and the emittance growth as a function of chromaticity, level of electron cloud density and bunch intensity. In the following section, the possibility to model the electron cloud effect with a broadband impedance [3] will be discussed and the results will be compared with the PIC simulations. Finally, the last section summarizes the results and draws an outline for future work and development.

HEADTAIL CODE AND THE NEW CONDUCTING BOUNDARY CONDITIONS

The code HEADTAIL for the single bunch instability has been described in Refs. [4], [5]. The simulation models the turn-by-turn interaction of a single bunch with an electron cloud, which is assumed to be produced by the preceding bunches and is taken to be initially uniform. Its density is inferred from parallel simulations with the ECLOUD code [6]. For the purpose of the simulation, the electron cloud is assumed to be concentrated at one or more Interaction Point (IP) around the ring and a fresh uniform electron distribution is created prior to each bunch passage. Both the protons and the electrons are represented by macroparticles and the bunch is also divided into longitudinal slices which enter into and interact with the cloud on successive time steps. The principle of the simulation is schematically illustrated in Fig. 1.

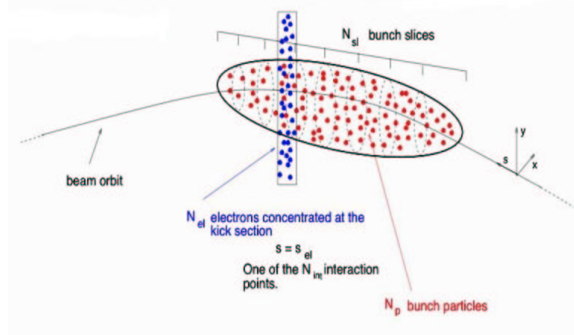


Figure 1: Schematic of the physical model for the cloud-beam interaction in HEADTAIL.

The transverse electrical interaction between the elec-

* DENER & INFN, Politecnico di Torino (Italy) and CERN

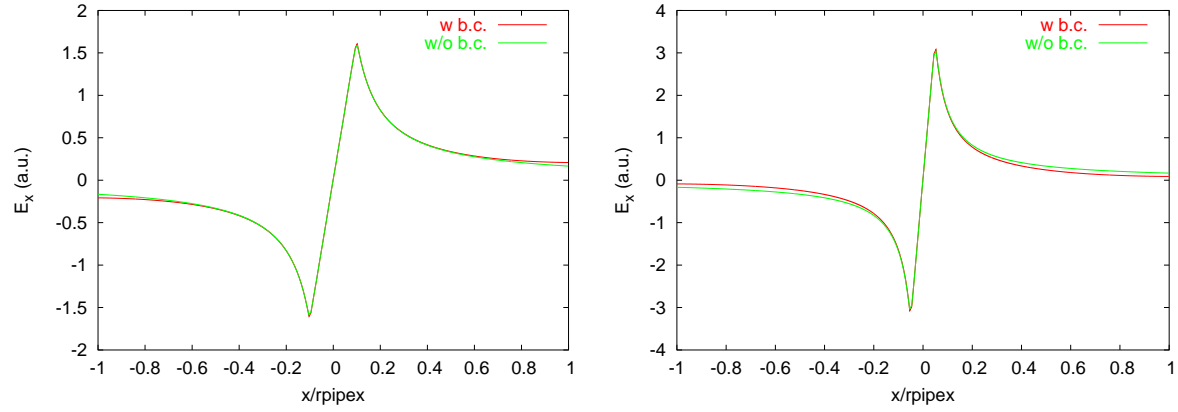


Figure 2: Horizontal electric field along the x-axis of a square (left) and rectangular box with $a = 2b$ (right), computed with and without conducting b.c. The vertical field is zero. The beam is in the centre of the chamber and $b = 10\sigma$.

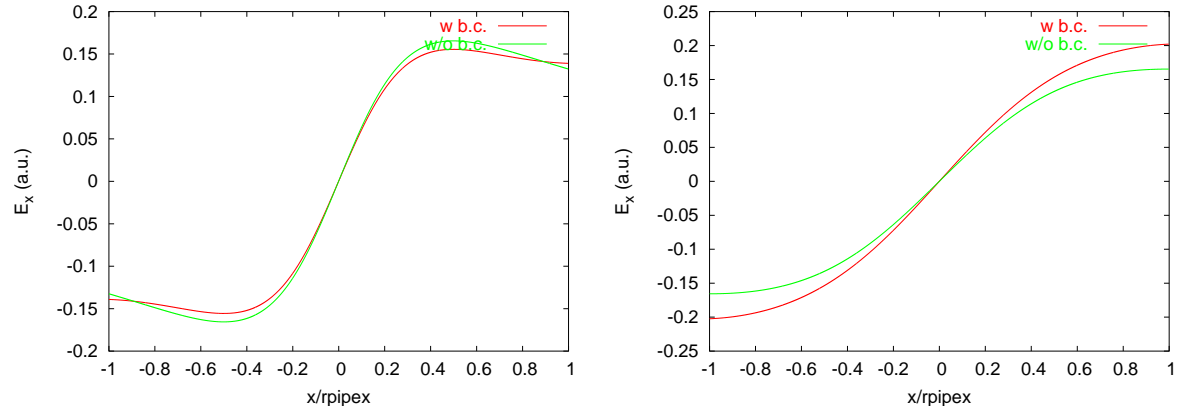


Figure 3: Horizontal electric field along the axis $y = \pm b/2$ of a square (left) and rectangular with $a = 2b$ (right), computed with and without conducting b.c.

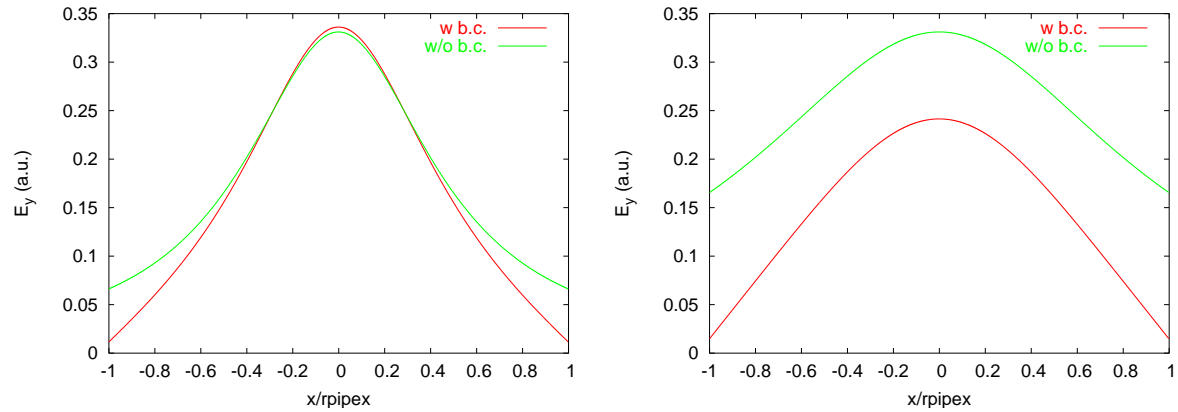


Figure 4: Vertical electric field along the axis $y = \pm b/2$ of a square (left) and rectangular with $a = 2b$ (right), computed with and without conducting b.c.

trons and the protons of each slice (and vice versa) is computed by a 2D PIC module. In between, the beam is transported around the ring, where the betatron motion in both planes is modelled by a rotation matrix. The synchrotron motion is included, so that the particles slowly mix longitudinally. In particular, they can move from one bunch slice to another during several turns. The effect of chromaticity is also modelled, via an additional rotation matrix. In the code there is the further possibility to include space charge and the effect of a broadband resonator. Feedbacks and various nonlinear fields are optionally available as well.

Recently new boundary conditions of a perfect electric conductor have been implemented, instead of the previous open space b.c. The potential is assumed to be zero on the wall and an FFT Poisson Solver for a rectangular pipe, based on sine transformations, has been used. The electric field is significantly different especially in the proximity of the boundary. Figure (2) shows the differences in the field on the x-axis between a small Gaussian beam in open space and in a square box or in a rectangular box with $a = 2b$ (being $a, b \gg \sigma_{x,y}$). Theoretical ratios on the pipe wall ($x = a, y = 0$), are expressed through the analytical formula:

$$\frac{E_{bc}}{E_{os}} = \sum_{m=0}^{\infty} \frac{(-1)^m}{2m+1} \quad (1)$$

$$+ 4 \sum_{m=0}^{\infty} \frac{(-1)^m}{2m+1} \sum_{n=1}^{\infty} \sin^2 \left[\arctg \left(\frac{2m+1}{n} \frac{a}{b} \right) \right] (-1)^n$$

resulting in

$$\left. \frac{E_{bc}}{E_{os}} \right|_{a=b} = 1.31 \quad \left. \frac{E_{bc}}{E_{os}} \right|_{a=2b} = 0.54 \quad , \quad (2)$$

which is very satisfactorily reproduced by our Poisson solver.

The difference between the electric field in open space and in a rectangular box becomes more critical as we move closer to the box wall in both directions. Figures 3 and 4 show both horizontal and vertical components of the electric field on a line $y = \pm b/2$. Fields can differ in this region by more than a factor 2.

SENSITIVITY TO NUMERICAL PARAMETERS

For the purpose of checking the sensitivity to simulation parameters we have performed a series of simulations for the LHC at injection. The bunch and numerical parameters which has been used are listed in Tables 1 and 2. In Fig.5 we show the vertical emittance vs. time for different numbers of electron macroparticles: a number of macroelectrons equal to 10^5 at every IP has been chosen in the following. If the cloud is initialized as a transversely uniform distribution inside the chamber, this correspond to about 6.1 macroparticles per cell (the number of grid points over $\pm 10 \sigma$ is 128). The number of macroparticles is taken to be 3×10^5 and the bunch has been divided into 70 slices.

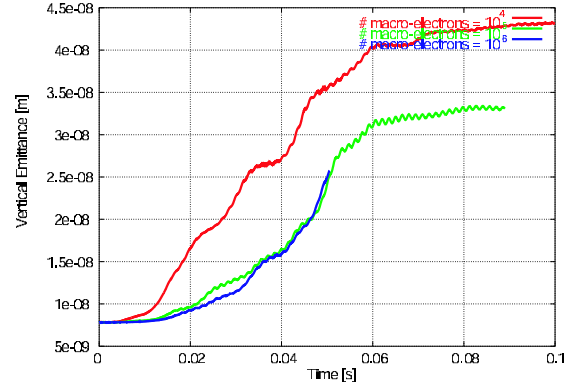


Figure 5: Emittance vs. time for different numbers of macroelectrons in the simulations.

Table 1: Parameters used in the simulations for LHC at injection

electron cloud density	ρ_e	$6 \times 10^{11} \text{ m}^{-3}$
bunch population	N_b	1.1×10^{11}
beta function	$\beta_{x,y}$	100 m
rms bunch length	σ_z	0.115 m
rms beam size	$\sigma_{x,y}$	0.884 mm
rms momentum spread	δ_{rms}	4.68×10^{-4}
synchrotron tune	Q_s	0.0059
momentum compaction fact	α_c	3.47×10^{-4}
circumference	C	26.659 km
nominal tunes	$Q_{x,y}$	64.28, 59.31
chromaticity	$Q'_{x,y}$	2, 2
space charge		no
magnetic field		no
linear coupling		no
dispersion	D	0 m
relativistic factor	γ	479.6
cavity voltage	V	8 MV
cavity harmonic number	h	35640

A key parameter which needs to be set carefully in the simulations is the number of Interaction Points per turn of the bunch with the cloud. Figure 6 shows the horizontal and vertical emittance vs. time for different numbers of IPs per turn. In the vertical plane there is clear evidence of two different regimes for a small numbers of IPs. Looking at the snapshot of the vertical bunch shape (Fig.7) in the case

Table 2: Computational parameters used in the simulations

# of macro-electrons	NEL	10^5
# of macro-protons	NPR	3×10^5
# of slices	$NBIN$	70
# of grid points	N	128×128
size of the grid	σ_g	$10 \sigma_{x,y}$

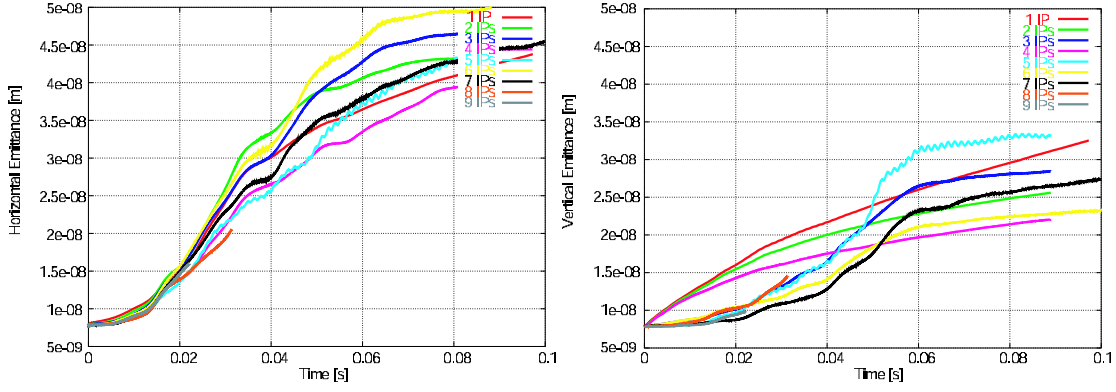


Figure 6: Horizontal (left) and vertical (right) emittance vs. time for different numbers of IPs, for LHC at inj, $\rho = 6 \times 10^{11} \text{ m}^{-3}$.

of only 1 point of interaction per turn the emittance growth appears incoherent and it occurs almost uniformly along the entire bunch, while in the case of 5 IPs the growth is due to an headtail instability. Hence, for the set of parameters listed in Tab.1, a number of IPs larger than 5 is required; in our simulations we have chosen $N = 10$.

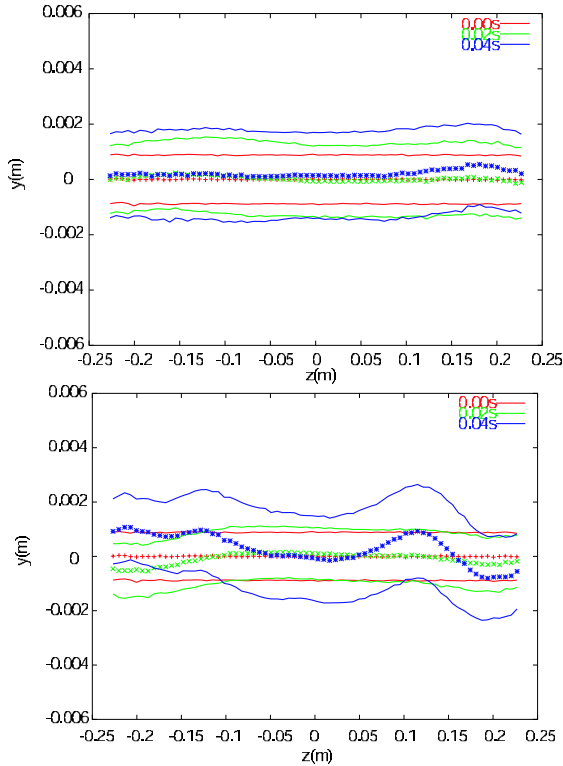


Figure 7: Snapshot of the vertical bunch shape (centroid and rms size) at different time step assuming 1 IP (top) and 5 IPs (bottom) per turn.

The location of the points of interaction along the ring and the phase advance between them is also important. In the code, the IPs are normally equally spaced and their position is fixed along the ring and does not change from turn to turn. Simulations were also performed by introducing

a random phase advance between IPs, where only the average number if IPs per turn is given, but their location and phase advance along the ring change every turn. Figure 8 shows that in this case for a small number of IPs the growth is larger than for a constant phase advance and that the convergence is very poor, but the change is monotonic and there is no evidence of two regimes. The larger growth is probably due to noise from the randomization.

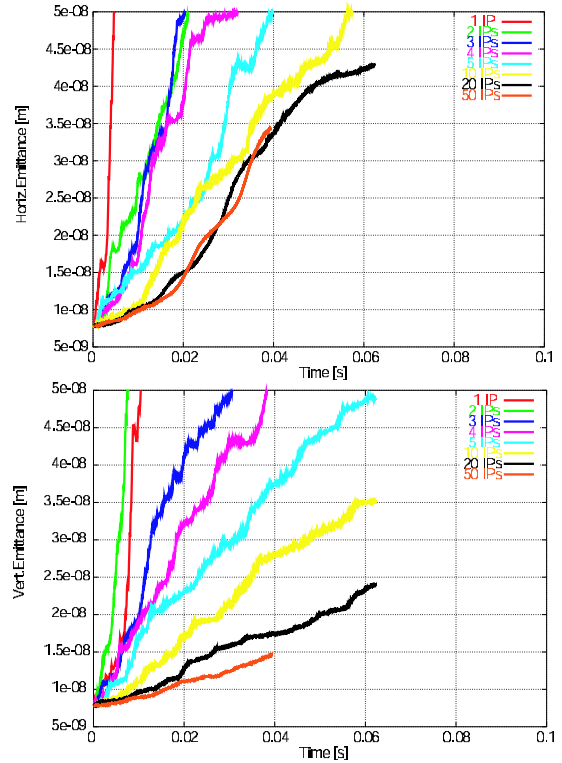


Figure 8: Random phase advance between IPs. Horizontal (top) and vertical (bottom) emittance vs. time for different numbers of IPs, for LHC at inj, $\rho = 6 \times 10^{11} \text{ m}^{-3}$.

The convergence of the simulation might be improved by concentrating the IPs in one betatron wavelength only [7]. Care should be taken since the distribution of RF cavities

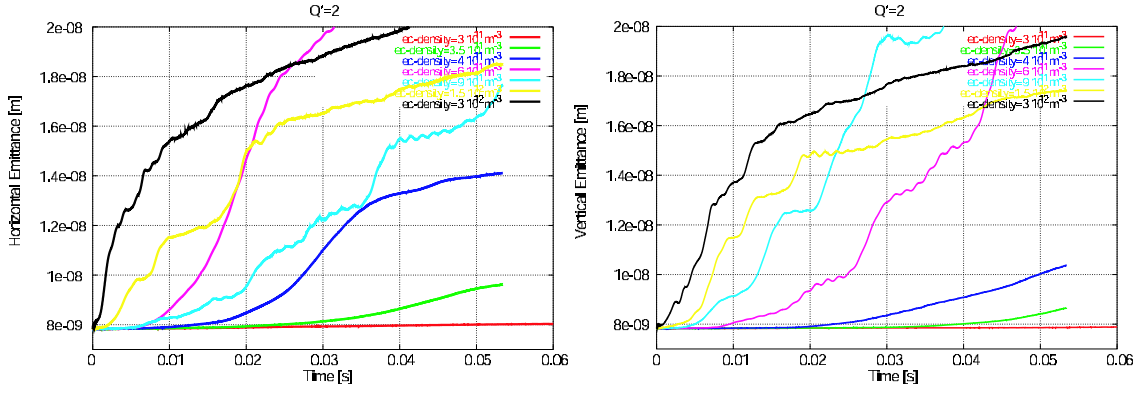


Figure 9: Horizontal (left) and vertical (right) emittance vs. time for different values of electron cloud density, in LHC at inj.

and regions with non-zero momentum compaction between interaction points may affect the instability behaviour as well [8].

INSTABILITY THRESHOLD AND EMITTANCE GROWTH IN LHC AT INJECTION

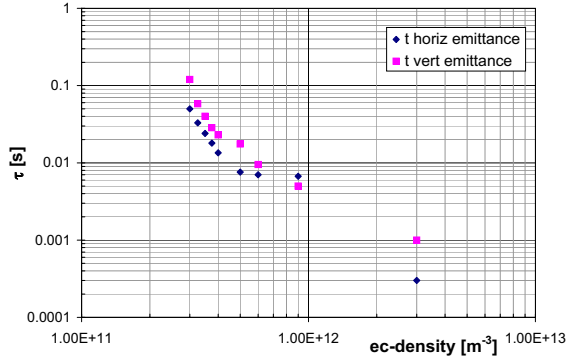


Figure 10: Rise time vs. cloud density. τ is the time during which the emittance increases from 7.82×10^{-9} m (initial value) to 8×10^{-9} m (+2.3%), in LHC at inj., $Q' = 2$

Using the parameters listed in Table 1, we studied the effect of chromaticity, electron cloud density and bunch intensity on the development of the instability, for the LHC at injection.

We first made a scan on the electron cloud density level in the chamber, from $3 \times 10^{12} \text{ m}^{-3}$ down to $2 \times 10^{11} \text{ m}^{-3}$. Figure 9 shows that for $\rho = 3 \times 10^{11} \text{ m}^{-3}$, only a very small slow emittance growth remains. This value is consistent with the threshold predicted by the analytical 2-particle model for the TMCI type instability [9]:

$$\rho^{thre} = \frac{2\gamma Q_s}{\pi r_p L \beta} \quad (3)$$

which gives $\rho = 4.31 \times 10^{11} \text{ m}^{-3}$ as a threshold for the fast headtail instability, for these parameters.

Figure 10 shows the emittance growth rise time as a function of electron cloud density level. Daring to extrapolate these 0.1 s simulations to 30 min operation in LHC at injection conditions, the maximum electron cloud density to keep the emittance growth lower than 2.3% is about $3 \times 10^{10} \text{ m}^{-3}$ which is at least one order of magnitude lower than the value permitted by heat-load considerations. But this result has of course to be interpreted with caution and in addition it has been obtained for zero chromaticity.

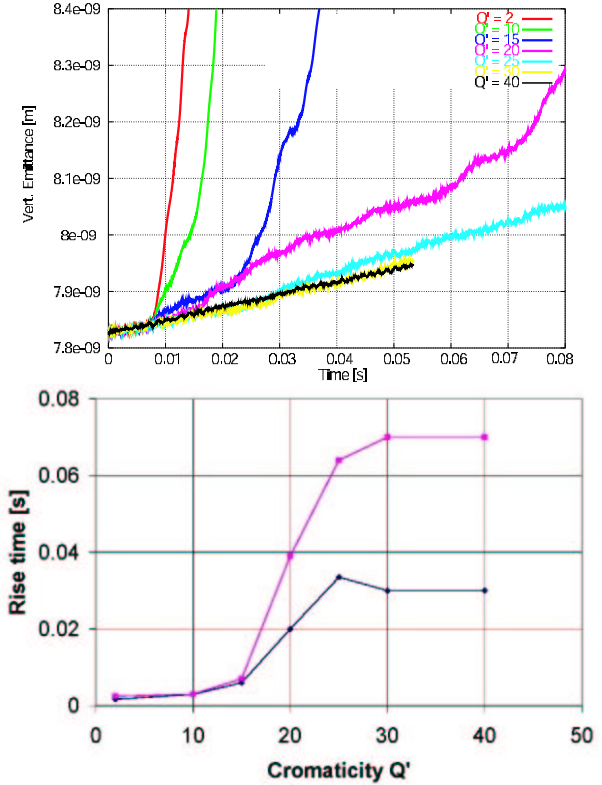


Figure 11: Vertical emittance growth for different chromaticities (top) and rise time vs Q' (bottom), in LHC at inj. Here the rise time is defined as the interval Δt in which the emittance passes from 8×10^{-9} m to 8.2×10^{-9} m

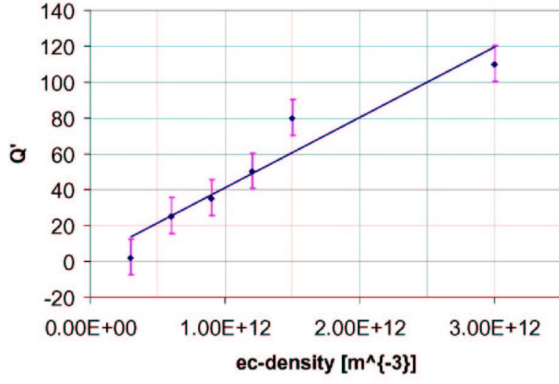


Figure 12: Chromaticity vs. electron cloud density at which the transition between the two regimes occurs, in LHC at inj.

Assuming an electron cloud density of $6 \times 10^{11} \text{ m}^{-3}$, increasing the chromaticity helps to reduce the emittance growth (Fig.11), until for very high values of $Q' = 30$ we enter in the other regime with a slow emittance growth. It is still to be proved that this slow emittance growth is not an artifact of the code (though similar growth has been seen in some measurements at KEKB [10]).

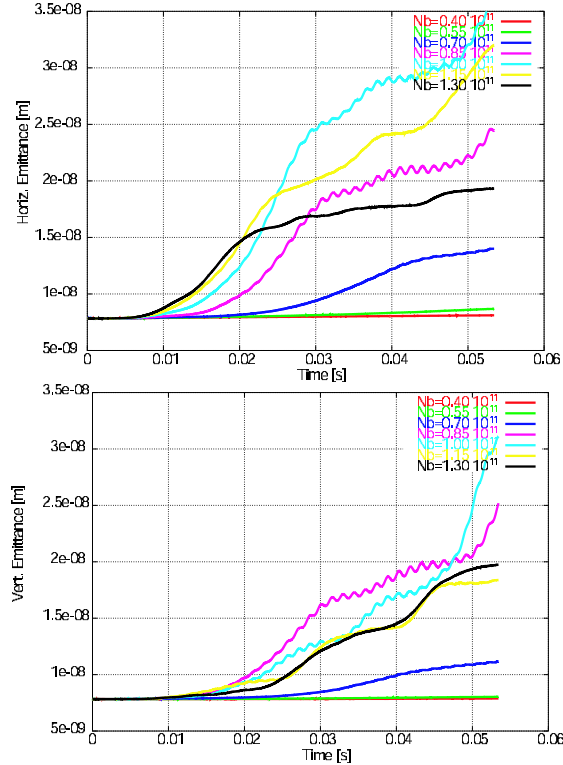


Figure 13: Horizontal (top) and vertical (bottom) emittance vs. time for different values of bunch intensities, for LHC at inj., $\rho = 6 \times 10^{11} \text{ m}^{-3}$.

The threshold value of chromaticity for which the strong headtail instability is cured depends on the electron cloud

Table 3: Parameters used in the simulations for LHC type beam in SPS

electron cloud density	ρ_e	10^{11} and 10^{12} m^{-3}
bunch population	N_b	1.1×10^{11}
beta function	$\beta_{x,y}$	40 m
rms bunch length	σ_z	0.24 m
rms beam size	$\sigma_{x,y}$	0.0021, 0.0021 mm
rms momentum spread	δ_{rms}	0.02
synchrotron tune	Q_s	0.0059
momentum compaction fact	α_c	1.92×10^{-3}
circumference	C	6911 km
nominal tunes	$Q_{x,y}$	26.185, 26.13
chromaticity	$Q'_{x,y}$	4.94, 3.9
space charge		no
magnetic field		strong field approx
linear coupling		no
dispersion	D	2.28 m
relativistic factor	γ	27.728
cavity voltage	V	2 MV
cavity harmonic number	h	4620

density. The relation found in our simulations (see Fig.12) is almost linear, as predicted by analytical computations for TMC Instability due to a broadband model [11].

A scan of the bunch intensity (Fig.13), for an electron cloud of $6 \times 10^{11} \text{ m}^{-3}$ and zero chromaticity, shows that for half the nominal bunch intensity we are below the strong headtail instability threshold and, at least for the first 50 ms, the emittance growth is strongly reduced.

HEADTAIL SIMULATION FOR SPS

Simulations have been done for LHC beam type in SPS. The parameters are listed in Tab.3. The aim of these simulations is benchmarking the code with observations.

In the SPS, the electron cloud is mainly concentrated in the bending magnets, and for this reason in the simulations the presence of a constant vertical magnetic field has been assumed, which causes the electron motion to be frozen in the horizontal plane (strong field approximation). The feedback system has also been implemented in the code, but it does not help a lot in reducing the single-bunch emittance growth because its main purpose is to cure the coupled-bunch instability and its bandwidth is too low to damp head-tail motion.

The scan in chromaticity for an electron cloud density of 10^{12} m^{-3} (Fig14) reveals that increasing the chromaticity only helps until a certain value of Q' . Also including space charge effects in the simulations drastically changes the results (see Fig.15). Figure16 show that for a lower level of electron cloud ($\rho = 6 \times 10^{11} \text{ m}^{-3}$) instead, even without space charge, the chromaticity significantly reduces the instability.

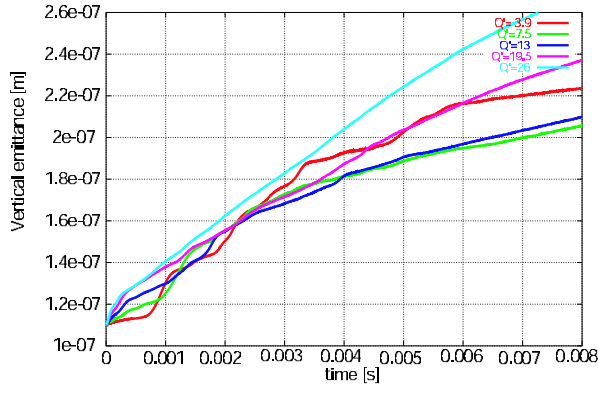


Figure 14: Vertical emittance vs. time for SPS, for different values of chromaticities, $\rho = 10^{12} \text{ m}^{-3}$.

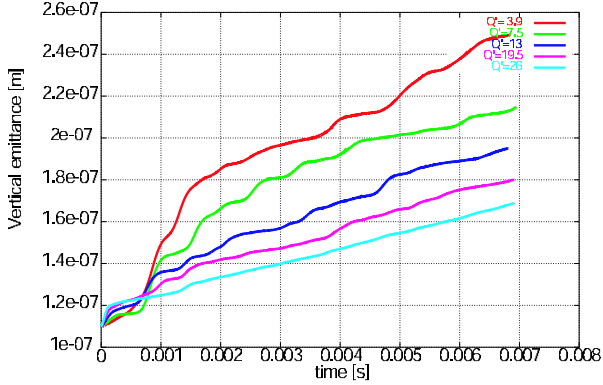


Figure 15: Vertical emittance vs. time for SPS, for different values of chromaticities, $\rho = 10^{12} \text{ m}^{-3}$. Space charge is included in the model.

BROADBAND IMPEDANCE MODEL FOR THE ELECTRON CLOUD

Results obtained by modelling the electron cloud by a resonator [3] with:

$$f_{res} = \frac{1}{2\pi} \sqrt{\frac{2r_e c^2}{2\sigma^2}} \sqrt{\frac{N_b}{\sqrt{2\pi}\sigma_z}} \frac{1}{\sqrt{k}} \quad (4)$$

$$\frac{cR_s}{Q} = H_{emp} \frac{\lambda_c r_e^{1/2}}{\sigma^3 k^{3/2} \sqrt{\frac{N_b}{\sqrt{2\pi}\sigma_z}}} L \quad (5)$$

have been compared with the PIC simulations in HEADTAIL. The quality factor is assumed to be $Q = 1$, σ is the transverse beam size, σ_z is the rms bunch length, λ_c is the cloud line density, N_b the beam intensity, L is the ring circumference, c is the light velocity, k is a coupling parameter and is taken equal to 2, and $H_{emp} = 0.4$ has been obtained empirically by matching against the PIC simulations. In HEADTAIL there is also the possibility to consider the effects of a broadband impedance. So simulations have been done using the resonator of (4) and (5) and compared with the results obtained using the PIC module.

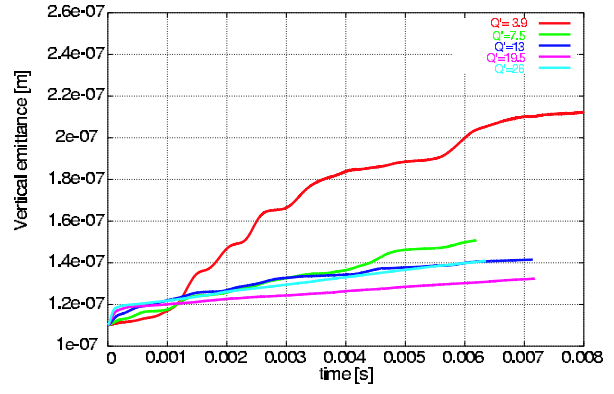


Figure 16: Vertical emittance vs. time for SPS, for different values of chromaticities, $\rho = 6 \times 10^{11} \text{ m}^{-3}$.

The resonator model seems to give similar growth rates as the full electron-cloud simulation (see Fig.17 and 18). For large amplitudes the finite size of the field grid and the non linear force slow down the emittance growth induced by the electron cloud in the case of the PIC calculation.

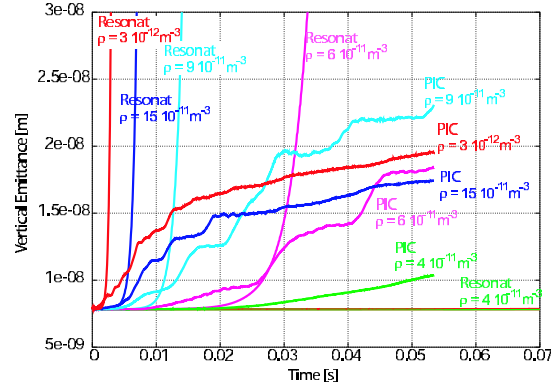


Figure 17: Emittance growth in LHC at injection, for different electron cloud density: comparison between the resonator model and HEADTAIL PIC module.

CONCLUSIONS AND OUTLOOK

The code HEADTAIL has been used to simulate single-bunch instabilities and emittance growth due to electron cloud in the LHC and SPS rings. Electrical conducting boundary conditions were added to replace the previous open space b.c. and sensitivity to numerical parameters has been checked. In particular we discussed the choice of the number and position of the Interaction Points between the bunch and the electron cloud, which in the code are assumed to be concentrated at a finite number of locations around the ring. Simulations for LHC at injection show that chromaticity is a cure for the strong headtail instability, but that it may not be efficient for suppressing a slow, long-term emittance growth. The question is still open whether this incoherent growth is real or if it is an artifact of the simulation. With zero chromaticity we are below the threshold

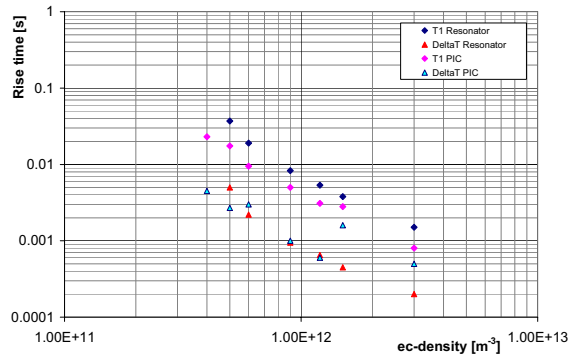


Figure 18: Rise time of the emittance growth vs. ec-density, in LHC at inj. T_1 is the time during which the emittance increases from 7.82×10^{-9} m (initial value) to 8×10^{-9} m, DeltaT is defined as the interval in which the emittance passes from 8×10^{-9} m to 8.2×10^{-9} m (+2.5%).

of the TMCI type instability up to half the nominal bunch intensity. With nominal parameters an electron density of $3 \times 10^{11} \text{ m}^{-3}$ must be achieved to stay below the threshold. Below this value there is still a slow emittance growth and, daring to extrapolate the results from 0.1 s to 30 min operation, an electron cloud level of only a few 10^{10} m^{-3} seems acceptable if the emittance growth due to the electron cloud should not exceed a few percent. The dependence on chromaticity has also been studied for the SPS. The results can be compared with observations. Here the space charge effect plays a key role.

The resonator model for the electron cloud and the PIC simulation seem to agree at the onset of the instability; later the non linear effects that are not taken into account in this model and the finite size of the cloud and of the grid used for the PIC computation become important and lead to a different behaviour at large amplitudes.

In the near-term future we are planning to benchmark the code against SPS experiments. The effect of the lattice on the emittance growth will also be studied and a collaboration is ongoing with USC, which aims to benchmark

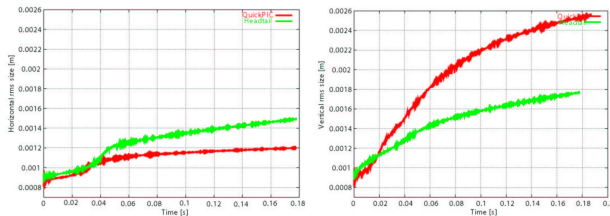


Figure 19: Horizontal(left) and vertical(right) emittance vs. time, for LHC at injection and $\rho = 6 \times 10^{11} \text{ m}^{-3}$. For purpose of comparison in both HEADTAIL (green line) and QuickPIC (red line) the electron cloud has been modeled using a single IP per turn. (QuickPIC results are courtesy of A. Ghalam.)

HEADTAIL with the continuous plasma code QuickPIC [12] and to explore the need to model the real lattice. Figure 19 shows a preliminary comparison between the two codes, using in both cases the single kick approximation.

ACKNOWLEDGEMENTS

The authors thank F. Ruggiero, G. Arduini, E. Metral, A. Ghalam, T. Katsouleas and K. Ohmi for helpful comments and discussions.

REFERENCES

- [1] G. Rumolo and F. Zimmermann, "Practical User Guide for HEADTAIL", SL-Note-2002-036 (2002)
- [2] E. Benedetto, G. Rumolo, F. Zimmermann, "HEADTAIL journal: updates and modifications", to be published
- [3] K. Ohmi, F. Zimmermann, E. Perevedentsev, "Wake field and fast head-tail instability caused by an electron cloud", Phys.Rev. E 65, 016502 (2002)
- [4] G. Rumolo, F. Zimmermann, "Theory and Simulation of the Electron-Cloud Instability", Proceedings of Chamonix XI, CERN-SL-2000-07 (DI)
- [5] G. Rumolo, F. Zimmermann, "Simulation of Single Bunch Instabilities Driven by Electron Cloud in the SPS", Proc. PAC'2001 Chicago, USA, and CERN-SL-2001-041 (AP) (2001)
- [6] G. Rumolo and F. Zimmermann, "Practical User Guide for ECLOUD", SL-Note-2002-016 (AP) (2002)
- [7] A. Chao et al., suggestion at this workshop
- [8] T. Raubenheimer, M. Pivi, private communication, May 2004
- [9] K. Ohmi, F. Zimmermann, "Head-Tail Instability Caused by Electron Clouds in Positron Storage Rings", Phys.Rev.Lett. 85, 3831 (2000)
- [10] H. Fukuma, these proceedings
- [11] E. Metral, "Stability Criteria for High-Intensity Single-Bunch beams in Synchrotrons", Proc. EPAC'02, CERN/PS 2002-022 (AE) (2002)
- [12] G. Rumolo, A.Z. Ghalam, T. Katsouleas et al., "Electron Cloud Effects on Beam Evolution in a Circular Accelerator", PRST-AB 6, 081002 (2003)